Alexandria Engineering Journal (2013) **52**, 249–257

Alexandria University

Alexandria Engineering Journal

www.elsevier.com/locate/aej
www.sciencedirect.com

ORIGINAL ARTICLE

Laminar natural convection in inclined rectangular cavities with a localized heat source

Samy M. Elsherbiny *, Emad H. Ragab

Mechanical Engineering Department, Faculty of Engineering, Alexandria University, Alexandria, Egypt

Received 26 July 2012; revised 28 February 2013; accepted 13 March 2013
Available online 16 April 2013

KEYWORDS

Natural convection;
Heat source;
Rectangular cavities;
Numerical methods;
Laminar convection

Abstract The paper investigates numerically laminar natural convection in inclined rectangular cavities with a localized heat source. A mathematical model was constructed where the conservation equations governing the mass, momentum, and thermal energy together with their boundary conditions were solved. The calculation grid used in the solution is investigated to determine the best grid spacing, the required number of iterations, and other parameters which affect the accuracy of the generated solutions. The numerical method and computer program were tested for the case of pure conduction to assure validity and accuracy of the numerical method.

The numerical investigation used air as the fluid and covered Rayleigh numbers based on scale length, s/A ranging from 10^2 to 10^6, aspect ratio from 0.5 to 5, position ratio from 0.25 to 0.75, heater size ratio from 0.25 to 1, and the tilt angle measured from horizontal was varied from 0 to 180°. The results are presented graphically in the form of streamline and isotherm contour plots. The heat transfer characteristics, velocity profiles, local and average Nusselt numbers were also presented. A correlation was developed which represents the present numerical heat transfer results with an average deviation of less than 11.5%.

1. Introduction

The natural convection in a differentially heated enclosure has been studied in the past both analytically and experimentally. Extensive survey on natural convection from a discrete heater in an enclosure is given by Chu and Churchill [1]. They examined the effect of the heater location in an enclosure where $A = 0.4$–0.5, $\mathrm{Pr} = 0.72$, $\Phi = 90°$ and for a range of Rayleigh number, Ra_H from 0 to 10^5. They found that the Nusselt number, Nu_H, was proportional to Ra_H for any location of the discrete heat source. Turner and Flack [2,3] have experimentally examined the heat transfer in geometry similar to that used by Chu and Churchill [1] for Grashof numbers up to 9×10^6. They obtained the same form for the correlation as $\mathrm{Nu}_H = \mathrm{C1} \cdot \mathrm{Gr}_H^{\mathrm{C2}}$ Where $\mathrm{Nu}_H = \frac{hH}{k}$, $\mathrm{Gr}_H = \frac{g\beta(T_h - T_c)H^3}{\nu^2}$ and C1 and C2 are functions of size ratio, ε. Yovanovich [4] reported

* Corresponding author.
E-mail address: samymelsherbiny@yahoo.com (S.M. Elsherbiny).

Peer review under responsibility of Faculty of Engineering, Alexandria University.

ELSEVIER Production and hosting by Elsevier

1110-0168 © 2013 Production and hosting by Elsevier B.V. on behalf of Faculty of Engineering, Alexandria University.
http://dx.doi.org/10.1016/j.aej.2013.03.001

Nomenclature

A	aspect ratio of enclosure, $A = H/L$
b	distance from $x = 0$ to center of heater, m
B	position ratio, $B = b/H$
C_p	specific heat at constant pressure, J/(kg K)
g	gravitational acceleration, m/s^2
Gr	Grashof number, $\mathrm{Gr} = g\beta\,(T_h - T_c)\,(s/A)^3/\nu^2$
h	average heat transfer coefficient, W/m^2 K
H	width of enclosure, m
k	thermal conductivity, W/m K
L	height of enclosure, m
Nu	average Nusselt number, $h(s/A)/k$
Nu_x	local Nusselt number, $h_x(s/A)/k$
p_d	dynamic pressure, N/m^2
P_d	nondimensional dynamic pressure, $P_d = p_d(s/A)^2/\rho\alpha^2$
Pr	Prandtl number, $\mathrm{Pr} = \mu C_p/k$
r_c	constriction resistance, K/W
Ra	Rayleigh number based on (s/A), $\mathrm{Ra} = g\beta\,(T_h - T_c)\,(s/A)^3/\nu\alpha$
s	length of discrete heat source, m
T	local fluid temperature, K
u	dimensional velocity component in x-direction, m/s
U	nondimensional velocity component in X-direction, $U = u\,(s/A)/\alpha$
v	dimensional velocity component in y-direction, m/s
V	nondimensional velocity component in Y-direction, $V = v\,(s/A)/\alpha$
x	dimensional coordinate, m
X	nondimensional coordinate, $X = x/(s/A)$
y	dimensional coordinate, m
Y	nondimensional coordinate, $Y = y/(s/A)$

Greek symbols

α	thermal diffusivity, $k/\rho\,C_p$, m^2/s
β	coefficient of volumetric thermal expansion, K^{-1}
ρ	local density, kg/m^3
μ	dynamic viscosity, kg/m s
ν	kinematic viscosity, $\nu = \mu/\rho$, m^2/s
Φ	angular coordinate, rad
θ	dimensionless temperature, $\theta = (T - T_c)/(T_h - T_c)$
ε	Plate size ratio, s/H

Subscripts

c	cold
h	hot

an expression for the thermal constrictive resistance of a discrete heat source on a rectangular solid region with the heat sink on the opposite side and other sides are assumed insulated. The expression is given as $r_c = (1/\pi k)\ \ln\ [(1/\sin(\pi\varepsilon/2)\cos\pi\ (B{-}0.5)]$.

ElSherbiny [5] determined experimentally the effect of heater location (full contact heat source, $\varepsilon = 1$) using three heaters on the hot wall. He measured Nu for each heater and found that Nu for upper heater was decreased up to certain Ra and then increased. Markatatos and Periclous [6] have experimentally examined the heat transfer in a square enclosure ($A = 1$), full contact heated wall ($\varepsilon = 1$), $\mathrm{Pr} = 0.71$, $\Phi = 90°$, $B = 0.50$, and the range of Ra from 10^3 to 10^{12}. They obtained the velocity distribution and a correlation of Nusselt number as a function of Ra_H as $\mathrm{Nu}_H = \mathrm{C1} \times (\mathrm{Ra}_H)^{\mathrm{C2}}$, where C1 and C2 depend on Ra_H. Keyhani et al. [7] have experimentally studied the heat transfer in an enclosure filled with ethylene glycol. The hot wall consisted of 11 discrete isoflux heaters where $A = 16.5$, $\mathrm{Pr} = 150$, and the local modified Rayleigh number is in the range of 9.3×10^{11} to 1.9×10^{12}. They correlated the local Nusselt number as $Nu_x = 1.009 \cdot \mathrm{Ra}_x^{0.1805}$, where "$x$" is the local height, measured from bottom of cavity to midheight of the heated section.

Chadwick et al. [8] have experimentally examined the heat transfer in a rectangular enclosure with an isoflux heating mode where $A = 5$, $\mathrm{Pr} = 0.71$, $\varepsilon = 0.133$, $\Phi = 90°$, and Gr^* range of $10^4 \leqslant \mathrm{Gr}^* \leqslant 5 \times 10^5$. They obtained the value of average Nusselt number as a function of Gr^* based on heater length $\mathrm{Gr}^* = g\beta s^4/k\nu^2$. The average Nusselt number was obtained by $\mathrm{Nu} = \mathrm{C1} \times (\mathrm{Gr}^*)^{\mathrm{C2}}$, where C1 and C2 are functions of "ε." Also, they obtained the value of local Nusselt number as a function of Gr_x^*, the local modified Grashof number based on distance from leading edge of heater $\mathrm{Gr}_x^* = g\beta x^4/k\nu^2$, and "$x$" is the distance from the leading edge of the heater to any point at heater surface. The local Nusselt number, Nu_x, was obtained by correlation $\mathrm{Nu}_x = \mathrm{C1} \times (\mathrm{Gr}_x^*)^{\mathrm{C2}}$,where C1 and C2 are functions of B. Ho and Chang [9] studied numerically and experimentally the influence of aspect ratio on heat transfer in an enclosure which has four isoflux heaters where A changes from 1 to 10, $\mathrm{Pr} = 0.71$, $\Phi = 90°$, and a range of Ra_H^* from 10^4 to 10^6. They obtained the value of Nu_H as $\mathrm{Nu}_H = \mathrm{C1} \times (\mathrm{Ra}_H^*)^{\mathrm{C2}} \times \mathrm{A}^{\mathrm{C3}}$, where C1, C2, and C3 are constants which depend on heater arrangement.

Heindel et al. [10,11] have experimentally studied the heat transfer in a rectangular enclosure. The heat wall consisted of 3×3 array of heaters where $\Phi = 90°$, A ranges from 2.5 to 7.5, Pr ranges from 5 to 25, and Ra_L ranges from 10^5 to 10^8. They obtained the value of Nu for each row of heaters as $\mathrm{Nu} = \mathrm{C} \times \mathrm{Ra}^{0.25}$ where C is a function of row arrangement.

Ahmed and Yovanovich [12] studied numerically the influence of discrete heat source location on natural convection heat transfer in a range of Ra, based on scale length, s/A from 0 to 10^6, $\mathrm{Pr} = 0.72$, $A = 1$, $B = 0.5$, and $0 \leqslant \varepsilon \leqslant 1.0$. They obtained analytical correlations for this problem for either isothermal heat source or isoflux heat source as:

(a) For isoflux discrete heat source

$$\text{for } 0 \leq \mathrm{Ra}^* \leq 10^6\varepsilon^4 \quad \mathrm{Nu} = \left[\varepsilon^{1.511} + \left(0.21\varepsilon^{-0.288}(\mathrm{Ra}^*)^{0.221}\right)^{(17/2)}\right]^{(2/17)}$$

$$\text{for } 10^5 \leqslant \mathrm{Ra}^* \qquad \mathrm{Nu} = \varepsilon^{0.2} + 0.0302(\mathrm{Ra}^*)^{0.35}$$

(b) For isothermal discrete heat source

$$\text{for } 0 \leqslant \mathrm{Ra}^* \leq 10^6\varepsilon^3 \quad \mathrm{Nu} = \left[\varepsilon^{1.7} + (0.146\varepsilon^{-0.256}(\mathrm{Ra})^{0.287})^{(17/2)}\right]^{(2/17)}$$

$$\text{for } 10^5 \leqslant \mathrm{Ra}^* \qquad \mathrm{Nu} = \varepsilon^{0.2} + 0.0558(\mathrm{Ra}^*)^{0.35}$$

Al Bahi et al. [13] studied numerically the effect of heater location on local and average heat transfer rates in an enclosure which has a single isoflux heater where $A = 1$, $\mathrm{Pr} = 0.71$, $\Phi = 90°$, $\varepsilon = 0.125$, Ra^* ranges from 10^3 to 10^6, and $B = 0.25, 0.50$, and 0.75. They obtained isotherms, streamlines, and temperature distribution characteristics at high and low Ra^*. Al Bahi et al. [14] studied numerically the effect of tilt angle from horizontal on local and average heat transfer rates in an enclosure which has a single isoflux heater where $A = 5$, $B = 0.50$, $\varepsilon = 0.125$, Φ is varied from 0° to 180°, $\mathrm{Pr} = 0.71$, and Ra^* ranges from 10^2 to 10^6. They obtained isotherms and streamlines plots for different Ra^*. Sezai and Mohamed [15] studied numerically the effect of heater size ratio on average heat transfer rates in a rectangular enclosure which has a single heater where, $\Phi = 0°$, $0 \leqslant \varepsilon \leqslant 1$, $\mathrm{Pr} = 0.71$ and Rayleigh numbers based on enclosure height, $\mathrm{Ra}_L \geqslant 10^3$. They found that Nu was decreased when ε increased. Aydin and Pop [16] studied numerically the effect of heater size, Rayleigh number, Prandtl number on heat transfer rate in an enclosure where $\Phi = 90°$ and $B = 0.50$. They presented the results in the form of isotherms and streamlines plots as well as the variation of the local Nusselt number through the discrete heater.

Saeid and Pop [17] studied numerically the effect of heater size, location, and aspect ratio on heat transfer rate in a porous cavity saturated with water which possesses a density maximum in the vicinity of 3.98 °C, where $\Phi = 90°$ and $50 \leqslant \mathrm{Ra} \leqslant 1000$. They found that for long heater and low Ra, the maximum heat transfer occurs when $B = 0.50$. For short heater and high Ra, fixing the heater in the upper half of the vertical wall leads to an enhancement of the heat transfer. Also, increasing A more than 0.50, Nu will be increased.

Saeid [18] studied numerically the influence of discrete heat source location on natural convection heat transfer in a range of Ra from 10 to 10^3, $A = 1$ and $0.1 \leqslant \varepsilon \leqslant 0.50$. They found that the maximum average Nusselt number takes place when the heater is placed near the bottom of the vertical wall for high values of Ra and relatively higher location for relatively low values of Ra for both isothermal or isoflux heat source. Bae et al. [19] studied numerically the effect of number of heaters (full contact heat source, $\varepsilon = 1$) where $10^4 \leqslant \mathrm{Ra} \leqslant 10^8$. They found that, at low Ra, heat transfer across the enclosure is strengthened as the number of heaters increases. Corvaro and Paroncini [20] studied numerically and experimentally the effect of heater location where $A = 1$ and $\mathrm{Pr} = 0.71$ using three heaters on the hot wall. They measured temperature distribution and Nusselt numbers at different Rayleigh numbers on the heated strip.

Ramadhyani and Incropera [21] have experimentally determined the heat transfer coefficient for various flow rates, fluids, heater sizes, and enclosure dimensions. Jin et al. [22] studied numerically the effect of slowly rotating an enclosure (about its longitudinal horizontal axis) with three rows of discrete heat sources on Nu and heat transfer where $A = 3.75$, 7.5, $10^3 \leqslant \mathrm{Ra}^* \leqslant 10^7$, and $\mathrm{Pr} = 0.71$. They found that heat transfer behavior for the heaters of rows 1 and 3 is asymmetrical. Choi and Ortega [23] studied numerically the effect of inlet flow velocity and the inclination angle on Nu and heat transfer where $\mathrm{Pr} = 0.71$. They found that Nu strongly depends on the inclination angle in natural and forced regimes. Papanicolaou and Gopalakrishna [24] studied numerically the effect of aspect ratio, heater size ratio, and Rayleigh number on Nu and heat transfer for isoflux discrete heating where $\mathrm{Pr} = 0.71$ and $\Phi = 0$. They found that the value of Nu depends on aspect ratio, size ratio, and Rayleigh number for single and multiple heaters. Yucel et al. [25] studied numerically the effect of aspect ratio, size ratio, inclination angle, and Rayleigh number on Nu where $0 \leqslant \Phi \leqslant 90°$, $0.1 \leqslant \varepsilon \leqslant 1.0$ and $5 \leqslant A \leqslant 20$ and $10^3 \leqslant \mathrm{Ra} \leqslant 10^5$. They obtained isotherms, streamlines, and temperature distribution characteristics for different Ra.

2. Mathematical model

The configuration under consideration is shown schematically in Fig. 1.

The fluid in an enclosure will be considered a Newtonian constant property fluid except for the density in the buoyancy force components existing in the momentum equations. The Boussinesq approximation will relate the variable density to the local temperature. In other words, the two momentum equations will be coupled with the energy equation. The differential equations governing the conservation of mass, momentum, and thermal energy are given as:

$$\frac{\partial u}{\partial x} + \frac{\partial v}{\partial y} = 0 \tag{1}$$

$$\rho\left(u\frac{\partial u}{\partial x} + v\frac{\partial u}{\partial y}\right) = \beta\rho g(T - T_c)\sin\phi - \frac{\partial p_d}{\partial x} + \mu\left(\frac{\partial^2 u}{\partial x^2} + \frac{\partial^2 u}{\partial y^2}\right) \tag{2}$$

$$\rho\left(u\frac{\partial v}{\partial x} + v\frac{\partial v}{\partial y}\right) = \beta\rho g(T - T_c)\cos\phi - \frac{\partial p_d}{\partial y} + \mu\left(\frac{\partial^2 v}{\partial x^2} + \frac{\partial^2 v}{\partial y^2}\right) \tag{3}$$

$$\left(u\frac{\partial T}{\partial x} + v\frac{\partial T}{\partial y}\right) = \alpha\left[\frac{\partial^2 T}{\partial x^2} + \frac{\partial^2 T}{\partial y^2}\right] \tag{4}$$

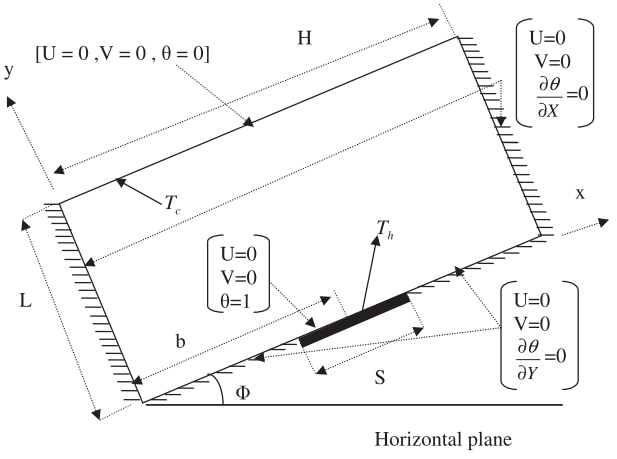

Figure 1 Boundary conditions of natural convection problem.

3. Dimensionless analysis

The mathematical set of equations, the continuity Eq. (1), the momentum Eqs. (2) and (3), and the energy Eq. (4) have to be solved numerically. In order to reduce the computational effort, it is first necessary to cast the set of equations in a dimensionless form. Introducing the following dimensionless variables:

$$X=\frac{x}{(s/A)},\quad Y=\frac{y}{(s/A)},\quad U=\frac{u(s/A)}{\alpha},\quad V=\frac{v(s/A)}{\alpha},$$
$$\theta=\left(\frac{T-T_c}{T_h-T_c}\right)$$

$$P_d=\frac{p_d(s/A)^2}{\rho\alpha^2},\quad \mathrm{Pr}=\frac{Cp\mu}{k},\quad \mathrm{Ra}=\frac{\left(\frac{s}{A}\right)^3\beta g(T_h-T_c)}{\nu\alpha}$$

where $\nu=\frac{\mu}{\rho}$, $\alpha=\frac{k}{c_p\rho}$

The dimensionless governing equations will result:

$$\frac{\partial U}{\partial X}+\frac{\partial V}{\partial Y}=0 \tag{5}$$

$$U\frac{\partial U}{\partial X}+V\frac{\partial U}{\partial Y}=\mathrm{RaPr}\theta\sin\phi-\frac{\partial P_d}{\partial X}+\mathrm{Pr}\left(\frac{\partial^2 U}{\partial X^2}+\frac{\partial^2 U}{\partial Y^2}\right) \tag{6}$$

$$U\frac{\partial V}{\partial X}+V\frac{\partial V}{\partial Y}=\mathrm{RaPr}\theta\cos\phi-\frac{\partial P_d}{\partial Y}+\mathrm{Pr}\left(\frac{\partial^2 V}{\partial X^2}+\frac{\partial^2 V}{\partial Y^2}\right) \tag{7}$$

$$U\frac{\partial \theta}{\partial X}+V\frac{\partial \theta}{\partial Y}=\frac{\partial^2\theta}{\partial X^2}+\frac{\partial^2\theta}{\partial Y^2} \tag{8}$$

The discrete heat source (heater plate) is heated at T_h, and the opposing wall is cooled to T_c. All other walls are assumed adiabatic. On all solid walls, the no slip condition of the fluid is assumed, so that fluid velocity components u, v have to be annihilated. Thus, the boundary conditions in terms of the dimensionless variables are given as follows:

(a) For lower surface

$$\text{at}\quad Y=0\quad\text{and}\quad 0\leqslant X\leqslant\frac{BA}{\varepsilon}-\frac{A}{2}\quad U=0,\quad V=0,\quad \frac{\partial\theta}{\partial Y}=0 \tag{9}$$

$$\text{at}\quad Y=0\quad\text{and}\quad \frac{BA}{\varepsilon}-\frac{A}{2}\leqslant X\leqslant\frac{BA}{\varepsilon}+\frac{A}{2}\quad U=0,\quad V=0,\quad \theta=1 \tag{10}$$

$$\text{at}\quad Y=0\quad\text{and}\quad \frac{BA}{\varepsilon}+\frac{A}{2}\leqslant X\leqslant\frac{A}{\varepsilon}\quad U=0,\quad V=0,\quad \frac{\partial\theta}{\partial Y}=0 \tag{11}$$

(b) For right and left surfaces

$$\text{at}\quad X=0\quad\text{and}\quad 0\leqslant Y\leqslant\frac{1}{\varepsilon}\quad U=0,\quad V=0,\quad \frac{\partial\theta}{\partial X}=0 \tag{12}$$

$$\text{at}\quad X=\frac{A}{\varepsilon}\quad\text{and}\quad 0\leqslant Y\leqslant\frac{1}{\varepsilon}\quad U=0,\quad V=0,\quad \frac{\partial\theta}{\partial X}=0 \tag{13}$$

(c) For upper surface

$$\text{at}\quad Y=\frac{1}{\varepsilon}\quad\text{and}\quad 0\leqslant X\leqslant\frac{A}{\varepsilon}\quad U=0,\quad V=0,\quad \theta=0 \tag{14}$$

The local Nusselt number, Nu_x is defined as: Nu_x

$$=\frac{h_x\left(\frac{s}{A}\right)}{k}=-\left(\frac{\left(\frac{s}{A}\right)}{T_h-T_c}\right)\frac{\partial T}{\partial y} \tag{15}$$

The average Nusselt number, Nu can be calculated by the following:

$$\mathrm{Nu}=\frac{h\left(\frac{s}{A}\right)}{k}=\frac{-1}{A}\sum\left(\frac{\partial\theta}{\partial Y}\right)\Delta X\ldots\quad\ldots(\text{on heater plate}) \tag{16}$$

The grid used in the numerical solution is uniform. The grid size in each of the x- and y-directions is fixed with different values in each direction.

Different grid meshes were tried to determine the best grid size, which gives the most accurate Nusselt Number, Nu, to be used as the numerical solution. Table 1 shows the effect of grid mesh size on the average Nusselt number for case of ($\mathrm{Ra}=10^4$, $A=1$, $B=0.5$, $\varepsilon=0.5$, and $\Phi=90°$). Increasing the number of nodes in x- and y-directions (L1, M1), more than 42 did not increase the accuracy of Nu more than 0.91%. Due to the large number of runs in the present study (over 330 runs) and the increased run time, it was decided that it is good enough to use the mesh size 42×42.

The spacing between nodes in x-direction (ΔX) was changed from 0.025 to 0.1. It is shown that $\Delta X=0.025$ is good enough to reach a reasonable accuracy. Fig. 2 gives the effect of the spacing between nodes in x-direction (ΔX) on the average Nusselt number for the case ($\mathrm{Ra}=10^4$, $A=1$, $B=0.5$, $\varepsilon=0.5$, and $\Phi=90°$).

4. Results

4.1. Streamlines and isotherms

Fig. 3 shows the effects of heater size and its location on the development of isotherms and streamlines for $A=1.0$, $\Phi=90°$, and $\mathrm{Ra}=10^2$ up to 10^6. The computed isotherms for all heater sizes and locations are clustered near the hot surface indicating boundary layers build up. The parallel isotherms away from the heater at low Rayleigh number, $\mathrm{Ra}\leqslant10^3$, indicate conduction dominated mode of heat transfer, though convection is developed in the layer adjacent to the

Table 1 Average Nusselt numbers for different grid meshes.

ΔX	L1 × M1	Average Nusselt number	% Deviation
0.10	22 × 22	3.696	5.6
0.05	42 × 42	3.531	0.91
0.033	62 × 62	3.506	0.2
0.025	82 × 82	3.499	0

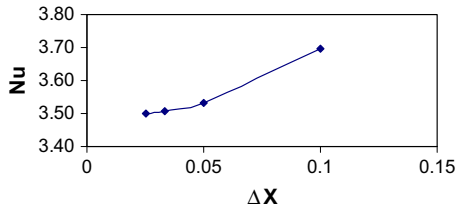

Figure 2 Effect of the spacing ΔX on average Nusselt number.

heating strip. The streamlines for all cases form a single vortex filling the cavity, and the effect of the heater size and location causes distortion of this cell. The form of distortion and the intensity of streamlines depend on size and location of heater and Rayleigh number.

As is seen from the isotherms in Fig. 3, at $Ra \leqslant 10^3$, weak convection is confined in the right side zone where the heat source is mounted. The parallel vertical isotherms for all heater positions reveal that the heat transfer across the enclosure is conduction dominated in particular within the region affected by the cold wall. Increasing Rayleigh number, up to $Ra = 10^6$, causes the convection heat transfer to be more confined along the heated vertical wall and the isotherms show thermal stratification in the core of the cavity.

4.2. Heat transfer

4.2.1. Effect of aspect ratio on Nusselt number

The effect of aspect ratio on Nusselt number in the vertical air layer is shown in Fig. 4 for $B = 0.50$ and $\varepsilon = 0.50$. It is shown that:

- For $A \leqslant 1.0$, the average Nusselt number, Nu increases with increasing A for low Rayleigh numbers, $Ra \leqslant 10^4$. However, Nu decreases for high Rayleigh numbers, $Ra > 10^4$.
- For $A > 1.0$, the average Nusselt number, Nu in general decreases with the increase in aspect ratio (the flow moves closer to conduction regime). However, this decrease in Nu increases with the increase in Ra.

4.2.2. Effect of position ratio on Nusselt number

The effect of position ratio on Nusselt number in a vertical air layer is studied for a size ratio, $\varepsilon = 0.5$ and different aspect ratios.

- **Case of ($A = 0.50$)**

Fig. 5 for aspect ratio, $A = 0.50$ shows that for low values of Rayleigh number, $Ra < 10^3$, the value of Nusselt number, Nu is nearly constant and independent of B. By increasing Ra, Nu is also increased. For $10^3 \leqslant Ra \leqslant 10^6$, the highest value of Nu occurs at position ratio, $B = 0.50$.

The main conclusion here is that maximum heat transfer can be achieved with the position ratio $B = 0.50$ (the heater is in the middle of the enclosure).

- **Case of ($A = 1.0$)**

Fig. 6 for aspect ratio, $A = 1.0$, shows that for $10^2 \leqslant Ra \leqslant 10^5$, the highest value of Nu happens at position ratio, $B = 0.50$ and for $10^5 \leqslant Ra \leqslant 10^6$, the highest value of Nu occurs at position ratio, $B = 0.25$.

- **Case of ($A = 5.0$)**

Fig. 7 for aspect ratio, $A = 5.0$, shows for $10^2 \leqslant Ra < 2.9 \times 10^4$, the highest value of Nu occurs at position ratio, $B = 0.50$ and for $Ra \geqslant 2.9 \times 10^4$, the highest value of Nu occurs at position ratio, $B = 0.25$.

The main conclusion here is that maximum heat transfer can be achieved with the position ratio $B = 0.25$.

4.2.3. Effect of size ratio on Nusselt number

The effect of plate size ratio on Nusselt number in a vertical air layer with $B = 0.5$ and different aspect ratios are explained as follows:

- **Case of ($A = 0.50$)**

Fig. 8 for aspect ratio, $A = 0.50$, shows that the value of Nusselt number highly depends on the size ratio. For $10^2 \leqslant Ra \leqslant 10^3$, the figure shows that increasing Rayleigh number, Ra increases Nu only for $\varepsilon = 0.25$. In general, the highest value of Nu occurs at the lowest value of size ratio ($\varepsilon = 0.25$). Increasing the size ratio from 0.25 to 1.0 has the effect of reducing the average Nusselt number, Nu for all values of Rayleigh number, Ra except for small range ($3.535 \times 10^5 \leqslant Ra \leqslant 10^6$) where the maximum Nu occurs at $\varepsilon = 0.50$.

- **Case of ($A = 1.0$)**

As shown in Fig. 9 for aspect ratio, $A = 1.0$, the same behavior of size ratio $A = 0.5$ occurred for $A = 1.0$. The highest Nu occurred at $\varepsilon = 0.25$ for all Ra values except for a small range ($3.5 \times 10^5 \leqslant Ra \leqslant 10^6$) where the maximum Nu occurred at $\varepsilon = 0.50$.

- **Case of ($A = 5.0$)**

Again, as shown in Fig. 10 for aspect ratio, $A = 5.0$, the highest average Nusselt number, Nu occurred at $\varepsilon = 0.25$ for all values of Ra. Increasing the size ratio ε from 0.25 to 1.0 leads to a reduction in Nu for all values of Ra.

4.2.4. Effect of inclination angle on Nusselt number

The effect of inclination angle, Φ on Nusselt number is shown in Fig. 11 for aspect ratio, $A = 1.0$, position ratio, $B = 0.50$, $\varepsilon = 0.50$. The angle Φ was changed from 0° to 180° with 15° steps. As is shown, the value of the Nusselt number is highly dependent on the inclination angle.

For $Ra = 10^2$, changing Φ from 0° to 180°, we found that the average Nusselt number, Nu, is nearly constant, and conduction regime is dominant.

For $10^3 \leqslant Ra \leqslant 10^5$, increasing inclination angle above $\Phi = 0$ will increase the average Nusselt number, Nu till angle, $\Phi = 75°$, and then, Nu will decrease up to $\Phi = 150°$. Nusselt number is nearly constant from $\Phi = 150°$ till $\Phi = 180°$.

For $Ra = 10^6$, increasing the inclination angle from $\Phi = 0$, we find that Nusselt number, Nu, will first decrease till $\Phi = 15°$ and then increase up to $\Phi = 75°$. Nusselt number,

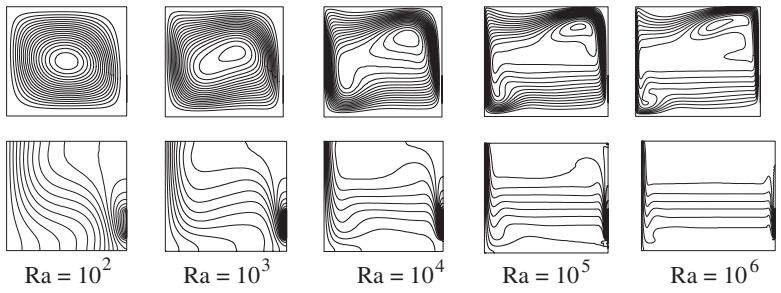

(a) B = 0.25, ε = 0.25

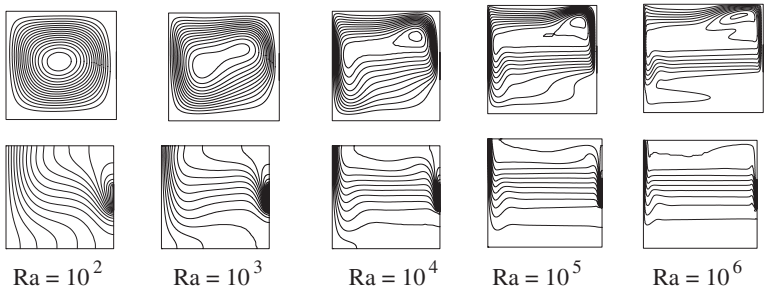

(b) B = 0. 50, ε = 0.25

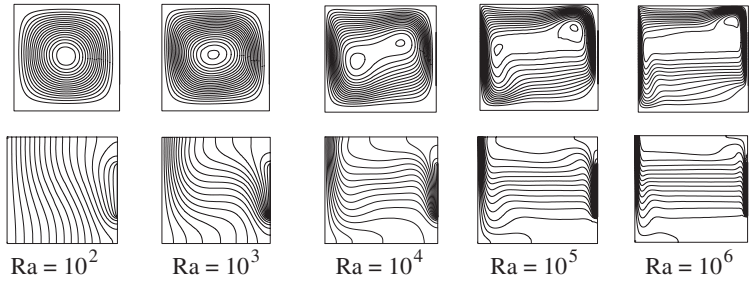

(c) B = 0.50, ε = 0.50

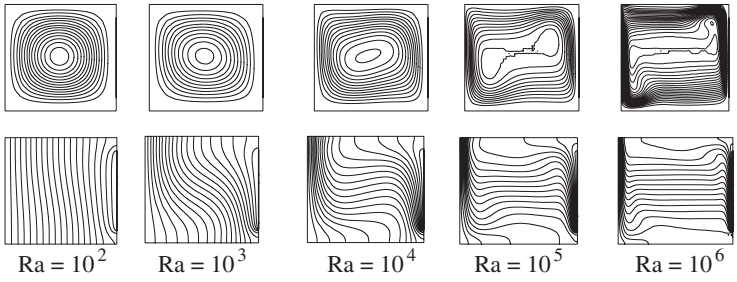

(d) B = 0.50, ε = 0.75

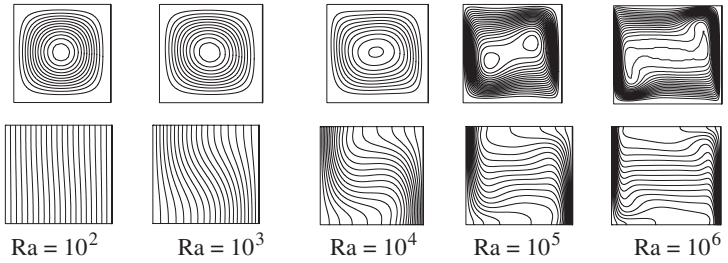

(e) B = 0.50, ε = 1

Figure 3 Streamlines (top) and isotherms (bottom) for vertical square air layers.

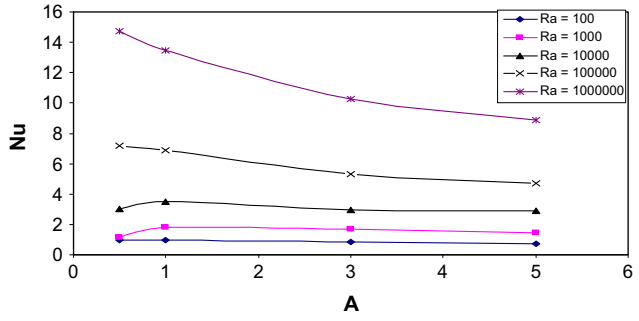

Figure 4 Effect of aspect ratio on average Nusselt number for ($B = 0.50$, $\varepsilon = 0.50$, $\Phi = 90°$, Pr = 0.72).

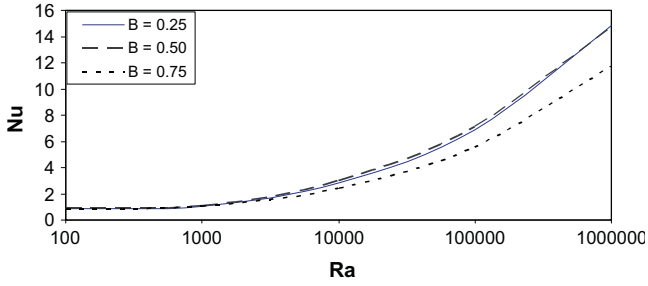

Figure 5 Effect of position ratio on average Nusselt number for ($A = 0.5$, $\varepsilon = 0.50$, $\Phi = 90°$, Pr = 0.72).

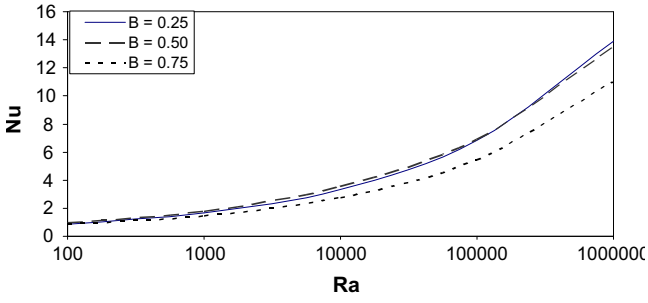

Figure 6 Effect of position ratio on average Nusselt number for ($A = 1.0$, $\varepsilon = 0.50$, $\Phi = 90°$, Pr = 0.72).

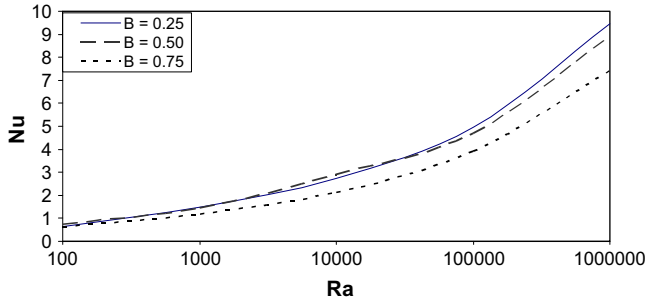

Figure 7 Effect of position ratio on average Nusselt number for ($A = 5.0$, $\varepsilon = 0.50$, $\Phi = 90°$, Pr = 0.72).

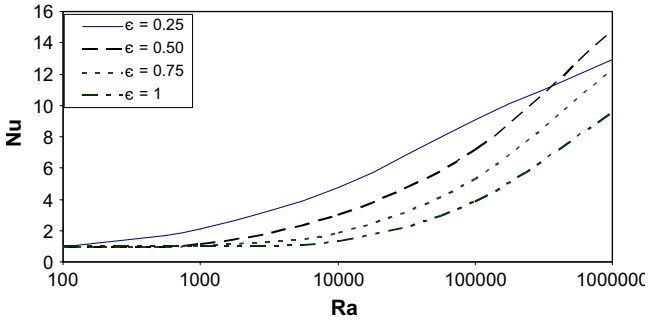

Figure 8 Effect of size ratio on average Nusselt number for ($A = 0.5$, $B = 0.50$, $\Phi = 90°$, Pr = 0.72).

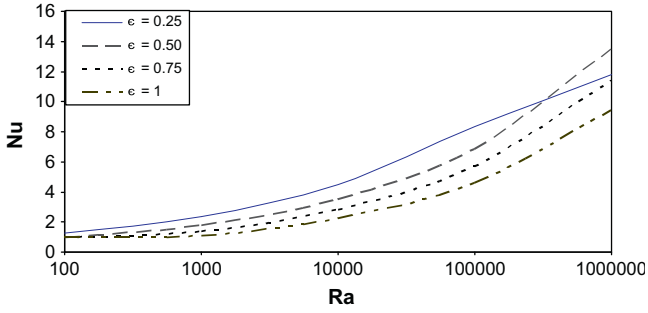

Figure 9 Effect of size ratio on average Nusselt number for ($A = 1.0$, $B = 0.50$, $\Phi = 90°$, Pr = 0.72).

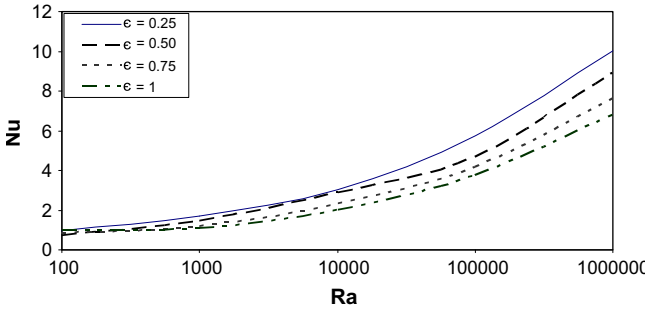

Figure 10 Effect of size ratio on average Nusselt number for ($A = 5.0$, $B = 0.50$, $\Phi = 90°$, Pr = 0.72).

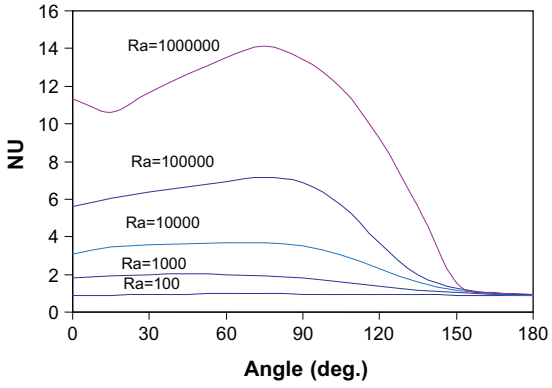

Figure 11 Effect of inclination angle on average Nusselt number for ($A = 1.0$, $B = 0.50$, $\varepsilon = 0.50$, Pr = 0.72).

Table 2 Constants used in equation.

Ra	C								
	$B + \varepsilon \leqslant 1$			$1 < B + \varepsilon < 1.5$			$B + \varepsilon = 1.5$		
	$A = 0.5$	$A = 1.0$	$A = 5$	$A = 0.5$	$A = 1.0$	$A = 5$	$A = 0.5$	$A = 1.0$	$A = 5$
10^2	0.045	0.85	0.027	0.042	0.05	0.05	0.01	0.1	0.1
10^3	0.077	0.12	0.055	0.026	0.065	0.041	0.045	0.055	0.053
10^4	0.123	0.13	0.086	0.056	0.086	0.060	0.032	0.07	0.061
10^5	0.129	0.126	0.079	0.084	0.089	0.058	0.06	0.07	0.058
10^6	0.1	0.1	0.07	0.0907	0.083	0.054	0.072	0.07	0.05

Table 3 Comparison with Ref. [12] ($B = 0.5$, Pr = 0.72 and $\Phi = 90°$).

No.	ε	Ra	Nu present	Nu Ref. [12]	% Deviation
1	0.25	10^2	1.284	1.103	14.1
2	0.50		0.962	1.029	−6.97
3	0.75		0.98	1.059	−8.06
4	1.0		1.001	1.103	−10.19
5	0.25	10^3	2.379	1.756	26.19
6	0.50		1.803	1.477	18.08
7	0.75		1.354	1.335	1.4
8	1.0		1.119	1.189	−6.26
9	0.25	10^4	4.479	3.514	21.55
10	0.50		3.531	2.665	24.53
11	0.75		2.843	2.665	6.26
12	1.0		2.26	2.176	3.72
13	0.25	10^5	6.877	5.476	20.37
14	0.50		5.698	4.805	15.67
15	0.75		4.628	4.442	4.02

Nu, will then decrease for $75° < \Phi < 150°$ and is nearly constant for $150° \leqslant \Phi \leqslant 180°$.

5. Correlations and comparison with previous work

For the case of air, Pr = 0.72, with $10^2 \leqslant \mathrm{Ra} \leqslant 10^6$, $A = 0.50$–5.0, $0.25 \leqslant B \leqslant 0.75$, $0.25 \leqslant \varepsilon \leqslant 1$ and tilt angle from horizontal, $\Phi = 90°$, a correlation was tried in the following form:

$$\mathrm{Nu} = B^{\varepsilon} + C \times \mathrm{Ra}^{0.35} \tag{17}$$

where C is constant given in Table 2 for different cases.

Eq. (17) is suitable for this case as a correlation and gave a maximum deviation of 15% except for few points.

The current work results were compared with the work published in Ref. [12] which presented results for the case of Pr = 0.72, $10^2 \leqslant \mathrm{Ra} \leqslant 10^5$, $A = 1.0$, $B = 0.50$, $0.25 \leqslant \varepsilon \leqslant 1$ and tilt angle from horizontal, $\Phi = 90°$.

The maximum deviation is found as 26% for few points and less than 15% for the majority of points. Table 3 shows the comparison.

6. Conclusions

The effect of several parameters on Nu was investigated and presented in form of graphs. For low Ra, the conduction regime is dominating in both isotherms and streamlines. Isotherms form parallel lines and streamlines form one cell filling the domain.

For high Ra, the flow changes to the boundary layer regime. Isotherms are concentrated on the surface of heater. Flow separation may occur due to pressure gradient.

It can be inferred that as Ra increases, Nu increases due to the concentration of isotherms on heater surface for higher Ra.

The aspect ratio, A affects Nu. As A increases, Nu decreases. This can be verified from Fig. 4. For lower Ra, Nu did not change much.

The position ratio, B affects Nu. For $A = 0.5$, $10^3 \leqslant \mathrm{Ra} \leqslant 10^6$, the highest value of Nu occurs at position ratio, $B = 0.50$ (the heater is in middle of the enclosure). For $A = 1.0$, $10^2 \leqslant \mathrm{Ra} \leqslant 10^5$, the highest value of Nusselt number, Nu, happens at position ratio, $B = 0.50$ and for $10^5 \leqslant \mathrm{Ra} \leqslant 10^6$, the highest value of Nu occurs at position ratio, $B = 0.25$. For $A = 5.0$, $10^3 \leqslant \mathrm{Ra} \leqslant 10^6$, the highest value of Nu occurs at position ratio, $B = 0.25$.

The heater size ratio ε also affects Nu. For $A = 0.5$ and 1.0, the highest value of Nu occurs at the lowest value of size ratio ($\varepsilon = 0.25$). Increasing the size ratio from 0.25 to 1.0 has the effect of reducing Nu for all values of Ra except for small range ($3.535 \times 10^5 \leqslant \mathrm{Ra} \leqslant 10^6$) where the maximum Nu occurs at $\varepsilon = 0.50$. For $A = 5.0$, the highest Nu occurred at $\varepsilon = 0.25$ for all values of Ra. Increasing the size ratio ε from 0.25 to 1.0 has the effect of reducing Nu for all values of Ra.

The tilt angle Φ also affects the Nu. For pure conduction, when Φ was changed, Nu is constant. For $10^3 \leqslant \mathrm{Ra} \leqslant 10^6$, increasing the tilt angle from $\Phi = 0$ will increase the average Nusselt number, Nu till angle, $\Phi = 75°$ and then Nu will decrease up to $\Phi = 150°$. Nusselt number is nearly constant

for $150° \leqslant \Phi < 180°$. For $Ra = 10^6$, increasing the inclination angle from $\Phi = 0$ will decrease Nu up to $\Phi = 15°$ and then will increase in the range $15° \leqslant \Phi < 75°$. Nu will then decrease till $\Phi = 150°$ and is nearly constant for $150° \leqslant \Phi \leqslant 180°$. The highest value of Nu occurs at $\Phi = 75°$.

A correlation was obtained for the vertical case with $Pr = 0.72$ and all studied values of Ra, A, B, and ε. It represented the data in a good way with an average deviation of 11.5%.

References

[1] H.H. Chu, S.W. Churchill, The effect of ratio and boundary conditions on two dimensional laminar natural convection in rectangular channels, ASME J. Heat Transfer. 98 (2) (1976) 194–201.

[2] B.L. Turner, R.D. Flack, Heat transfer correlations for use in naturally cooled enclosures with high-power integrated circuits, IEEE Trans. Compon., Hybr. Manuf. Technol. 3 (3) (1980) 449–452.

[3] R.D. Flack, B.L. Turner, Heat transfer correlations for use in naturally cooled enclosures with high-power integrated circuits, Manuf. Technol. 3 (3) (1980) 449–452.

[4] M.M. Yovanovich, Thermal conducting of a row of cylinders contacting two planes, in: AIAA 6th Thermodynamics Conference, Tullahoma, Tenn, 1971, pp. 307–315.

[5] S.M. ElSherbiny, Natural Convection Across Vertical Inclined Air Layers, Department of Mechanical Engineering. Springer Ltd., Berlin, 1980.

[6] N.C. Markatos, K.A. Pericleous, Laminar and turbulent natural convection in an enclosed cavity, Int. J. Heat Mass Transfer 27 (5) (1984), pp. 755–722.

[7] M. Keyhani, An experimental study of natural convection in a vertical discrete heat sources, ASME J. Heat Transfer 110 (1988) 616–624.

[8] M.L. Chadwick, B.W. Webb, H.S. Heaton, Natural convection from two-dimensional discrete heat sources in a rectangular enclosure, Int. J. Heat Mass Transfer 34 (1991) 1679–1693.

[9] C.J. Ho, J.Y. Chang, A study of natural convection heat transfer in a vertical rectangular enclosure with two-dimensional discrete heating, effect of aspect ratio, Int. J. Heat Mass Transfer 73 (6) (1994) 917–925.

[10] T.J. Heindel, S. Ramadhyani, F.P. Incropera, Laminar natural convection in a discretely heated cavity: I. Assessment of three-dimensional effects, ASME J. Heat Transfer 117 (1995), pp. 912–909.

[11] T.J. Heindel, S. Ramadhyani, F.P. Incropera, Laminar natural convection in a discretely heated cavity: II. Comparisons of experimental and theoretical results, ASME J. Heat Transfer 117 (1995) 910–917.

[12] G.R. Ahmed, M.M. Yovanovich, Influence of discrete heat source location on natural convection heat transfer in a vertical square enclosure, ASME J. Electron. Packag. 113 (1991) 268–274.

[13] A.M. Al Bahi, A.M. Radhwan, G.M. Zaki, Laminar natural convection from an isoflux discrete heater in a vertical cavity, Arabic J. Sci. Eng. 27 (2C) (2002) 149–164.

[14] A.M. Al Bahi, M.A.L. Hazmy, G.M. Zaki, Natural convection in a tilted rectangular enclosure with a single discrete heater, J. Eng. Sci. King Abdelaziz Univ., Jeddah, Saudi Arabia 16 (2) (2006) 141–167.

[15] I. Sezai, A.A. Mohamed, Natural convection from discrete heat source on the bottom of a horizontal enclosure, Int. J. Heat Mass Transfer 43 (13) (2000) 2226–2257.

[16] O. Aydin, I. Pop, Natural convection from a discrete heater in enclosures filled with a micropolar fluid, Int. J. Heat Mass Transfer 43 (19–20) (2005) 1409–1418.

[17] N.H. Saeid, I. Pop, Maximum density effects on natural convection from a discrete heater in a cavity filled with a porous medium, Acta Mech. 171 (3–4) (2004) 203–212.

[18] N.H. Saeid, Natural convection from a discrete heater in a square cavity filled with a porous medium, J. Porous Media 8 (1) (2005) 55–64.

[19] J.H. Bae, J.M. Hyun, H.S. Kwak, Buayant convection of variable. viscosity fluid in an enclosure with discrete protruding heaters, Int. J. Prog. Comput. Fluid Dyn. 5 (3–5) (2005) 144–151.

[20] F. Corvara, M. Paroncini, Temperature distribution; correlation distribution; nusselt number; numerical analysis; solar collectors; ventilation systems, J. Exp. Therm. Fluid Sci. 31 (31) (2007) 721–739.

[21] S. Ramadhyani, F. Incropera, Convection heat transfer from discrete source, Nat. Sci. Found. Award (1988).

[22] L.F. Jin, C.P. Tso, K.W. Tou, Natural convection heat transfer in a rotating enclosure with three rows of discrete heat source, J. Begell House 37 (2006) 395–405.

[23] C.Y. Choi, A. Ortega, Mixed convection in an inclined channel with a discrete heater, in: Conference on Thermal Phenomena in Electronic Systems, l. Therm lll, 1992, pp. 40–48.

[24] E. Papanicolaou, S. Gopalakrishna, Natural convection in shallow horizontal air layers encountered in electronic cooling, J. Electron. Packag. 117 (4) (1995) 307–316.

[25] C. Yucel, M. Hasnaoui, L. Robillard, E. Bilgen, Mixed convection heat transfer in open ended inclined channels with discrete isothermal heating, Numer. Heat Transfer Part A: Appl. 24 (1) (1993) 109–126.